Journal on Oncology

www.journalononcology.org

*Research Article*

***Open Access, Volume 3***

# *Does Liver MRI Require Intravenous Contrast Medium?*

***Izgi Berrin; Wenkel Evelyn; Saake Marc; Wetzel Matthias; Uder Michael; Janka Rolf****

*Radiologic Institute, Erlangen University Hosptial, Germany.*

## Abstract

**Purpose:** The aim of this study was to evaluate if and for which indications intravenous contrast medium (CM) is required in liver MRI.

**Material and methods:** The native sequences (T1w DIXON, T2w, T2w FS and DWI) of 240 consecutive liver MRI examinations were retrospectively evaluated by two radiologists in consensus. Sensitivity (SE), specificity (SP), positive predictive value (PPV) and negative predictive value (NPV) of the native sequences for the categories: no liver lesion, metastasis, HCC, cyst/hemangioma, FNH, adenoma and miscellaneous were determined.

**Results:** Native liver MRI was only convincing in the detection of liver metastasis (SE:100%, SP:100%, PPV:100%, NPV:100%). For all other entities, native MRI was inadequate, either in terms of sensitivity or specificity.

**Conclusions:** Native MRI provides reliable results for the detection of liver metastases and can therefore replace contrast-enhanced MRI (CE-MRI) for follow-up. For all other entities, CE-MRI cannot be omitted so far.

**Keywords:** Liver; MRI; Contrast media; Native; Liver lesions; Metastasis.

**Abbrevations:** CM: Contrast Media; MRI: Magnetic Resonance Imaging; DWI: Diffusion-Weighted Imaging; ADC: Apparent Diffusion Coefficient; RIS: Radiological Information System; LI-RADS: Liver Imaging Reporting and Data System; NEC: Neuroendocrine Carcinoma of the Gallbladder; CCC: Cholangiocellular carcinoma; SE: Sensitivity; SP: Specificity; PPV: Positive Predictive Value; NPV: Negative Predictive Value, HCC: Hepatocellular Carcinoma; FNH: Focal Nodular Hyperplasia; CE MRI: Contrast-Enhanced MRI.

## Introduction

In recent years MRI of the liver has established itself as the imaging technique with the greatest diagnostic accuracy. It is the method of choice for the diagnosis of liver malignancies [1], but also achieves good results in the characterization of benign liver lesions [2] or in the detection of liver metastases [3]. Therefore, MRI is the most important imaging modality for the detection of liver lesions besides ultrasound. In our institute at a tertiary care center, approximately 9% (1363/15932) of all MRI examinations in 2021 were MRI of the liver.

MRI of the liver is typically performed multiparametrically with i.v. contrast media (CM). Gadolinium-based contrast medias have recently been evaluated more critically because of nephrogenic systemic sclerosis and possible deposition in the brain and other organs [4,5]. Thus, the question arose whether and in which clinical scenario multiparametric liver MRI would achieve identical results without i.v. CM and thus CM administration could be omitted.

**Manuscript Information:** *Received: Sep 21, 2023; Accepted: Oct 25, 2023; Published: Oct 31, 2023*

**Correspondance:** *Janka Rolf, Radiologic Institute, Erlangen University Hosptial. Germany.*

*Tel: 4991318536065; Email: janka.rolf@uk-erlangen.de*

**Citation:** *Berrin I, Evelyn W, Marc S, Matthias W, Rolf J, et al. Does Liver MRI Require Intravenous Contrast Medium?. J Oncology. 2023; 3(2): 1111.*

## Material and methods

We retrospectively evaluated the native sequences from all consecutive liver MRIs of patients aged 19 years and older who were examined at our institute during a two-month period. If a patient was examined more than once during this period, only the first acquisition within the period was considered. All MRI examinations were performed on a 1.5 T scanner (MAGNETOM Aera, Siemens Healthcare GmbH, Erlangen, Germany). The MR protocol consisted of 5-6 pre-contrast sequences in transverse orientation and 5 mm slice thickness: T2w with and without fatty saturation, diffusion-weighted sequence with b values of 50,400, and 800, T1w DIXON, and a coronary T2w sequence with 5 mm slice thickness. The T2w sequence with fat saturation was primarily measured as a turbo spin echo sequence with respiratory triggering. If image quality was insufficient, a T2 HASTE sequence with fat saturation was added. The diffusion-weighted imaging (DWI) sequence was measured in free breathing with breath triggering.

After CM application (Gadovist single dose, Bayer, Berlin, Germany), three transverse T1w-VIBE DIXON sequences were measured in arterial, portal venous, and late phase, a transverse T1w FLASH sequence with fat saturation with a slice thickness of 5 mm, and a coronary T1w sequence with fat saturation and a slice thickness of 5 mm. The measurement parameters of the sequences can be found in Table 1. The pre-CM sequences of all MRI scans were re-analysed by two radiologists (B.I., resident with 1 year of experience and R.J., specialist/supervisor with many years of experience) in consensus. Both evaluators were blinded to post-CM measurements, patient history, diagnosis, and previous findings.

In the first step, all patients without lesions were identified (group 1). Patients with at least one lesion were classified by consensus of the two evaluators into metastasis (group 2), hepatocellular carcinoma (group 3), cyst or hemangioma (group 4), focal nodular hyperplasia (FNH) or adenoma (group 5) according to the criteria in Table 2. The criteria are based on the knowledge of the current literature [6]. The apparent diffusion coefficient (ADC) value of diffusion-weighted sequences was not considered because it is not valid for small lesions due to the potential difference in the respiratory position of each B-value measurement and the overlap area of the different lesions is too large [7]. If a clear classification into group 1 to 5 was not possible, the patients were assigned to group 6 (other) (Figure 1).

If more than one lesion was present, assignment to the more malignant group was made. For example, a case with hemangioma and hepatocellular carcinoma (HCC) was assigned to group 3. In routine clinical practice, all MRI evaluations, if available, use the information from the preliminary images and the patient's record/clinical information to make their findings. Therefore, in a 2$^{nd}$ step, we re-evaluated all lesions that could not be assigned so far (group 6) using the information from the radiological information system (RIS), the previous images and the electronic patient record ("second native analysis") (Figure 1). The lesions in group 2 (liver metastasis), group 3 (HCC), group 4 (cysts/hemangioma), and group 5 (FNH/adenoma) were additionally further analysed in terms of their number. More than 5 lesions were classified as "multiple lesions" and counted as 5 lesions in the analysis. Group 3 (HCC) lesions were evaluated after unblinding with all available sequences and prior imaging according to the Liver Imaging Reporting and Data System (LI-RADS) criteria [8]. The original report with all sequences - native and after contrast administration - served as reference and gold standard. Sensitivity, specificity, positive predictive value, negative predictive value, and accuracy of non-contrast images were calculated.

## Results

From 09/25/2021 to 11/24/2021, 259 liver MRIs were performed in our institute on 240 adult patients (159 male, 81 female) with a mean age of 42±17 years. The indications for these liver MRIs were:

-Exclusion of liver metastases in patients with known malignant tumour disease such as breast carcinoma, colorectal carcinoma, gastric carcinoma, pancreatic carcinoma, or neuroendocrine tumours (n=38).

-Follow-up of known liver metastases after medical treatment or after non-treatment (n=68). 12/68 patients had previous ablation therapy.

-Detection of malignant liver-derived tumours, e.g., early detection of hepatocellular carcinoma (HCC) in patients with liver cirrhosis or follow-up assessment of HCC with or without previous treatment/intervention (n=84).

-Further diagnostic clarification in case of clinically, laboratory-chemically or sonographically abnormal findings (n=50)

After evaluation of the precontrast images of all 240 MRIs, no lesions were found in 90 patients (in the original findings n=84, group 1). Liver lesions were detected in 150 patients (in original findings n=156, groups 2 to 6). Liver metastases were detected in 61 patients (in original report n=61, group 2), HCCs in 27 patients (in original report n=42, group 3), cysts/hemangiomas in 22 patients (in original report n=27, group 4), FNH/adenomas in 4 patients (in original report n=7, group 5). 36 patients could not be classified into groups 2 to 5 and were assigned to under the group "other" (in original findings n=19, group 6) (Figure 1; Table 3).

In the 36 patients with abnormal findings that could not be natively assigned to an entity, clinical information was included in the evaluation. With the help of information from RIS, previous images (CT or MRI with i.v. CM) and the electronic patient record, an entity of liver lesions could now be determined in 16 of 36 patients: HCC (n=6), hemangioma (n=3), adenoma (n=1), cholangiocellular carcinoma (CCC) (n=4), neuroendocrine carcinoma of the gallbladder (NEC) (n=1), and epithelioid hemangioendothelioma (n=1). The diagnoses of the remaining 20/36 patients were HCC (n=3), cyst (n=1), hemangioma (n=1), FNH (n=2), CCC (n=1, diagnosis after biopsy), ablation defect (n=5), angiosarcoma (n=1, diagnosis after biopsy), and unclear (n=6) in the original findings considering CM sequences and biopsy results (Figure 1).

In 6 patients with HCC, no lesion was detected in the native images and assigned to group 1 accordingly. Regarding the single-cell lesions, the results were as follows: In group 2 (liver metastases), all 268/268 lesions detected in the original findings could be identified as liver metastases in 61 of 61 patients (Table 4). In group 3 (HCC), 58/90 lesions were diagnosed as HCC in 33/42 patients (Table 4). The undetected 32/90 HCC lesions were classified as LI-RADS 3 in 13/35 (37%), LI-RADS 4 in 13/26 (50%), and

LI-RADS 5 lesions in 6/29 (21%) (Table 5). In group 4 (cyst/hemangioma), 104/106 lesions were identified as cyst or hemangioma in 25/27 patients (Table 4). In group 5 (FNH or adenoma), 3/5 lesions in 3/5 patients were detected as FNH and 10/10 lesions in 2/2 patients were detected as adenoma (Table 4). A detailed overview of the achieved SE(%), SP(%), PPV(%), NPV(%) and accuracy of the groups using native imaging is given in Table 6.

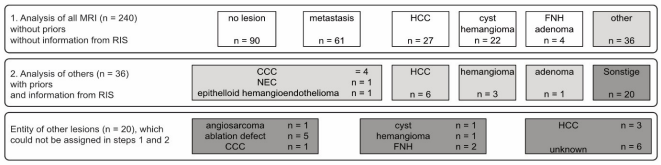


**Figure 1:** Flowchart of the evaluation of 240 MRIs.

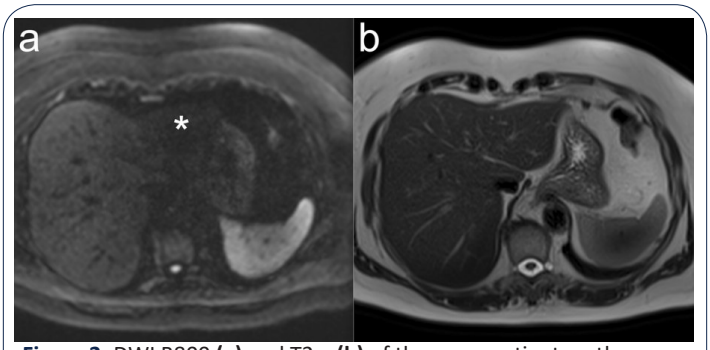


**Figure 2:** DWI B800 **(a)** and T2w **(b)** of the same patient on the same slice plane. Extinction phenomenon of the left hepatic lobe due to proximity to the heart in the DWI (star) compared to the T2w sequence.

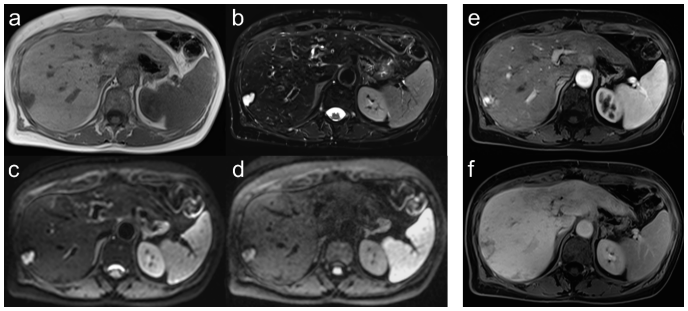


**Figure 3:** 59-year-old female patient with abnormal ultrasound findings in the right liver lobe. In the native sequences (**a:** T1w in-phase, **b:** T2w STIR, **c:** DWI B50, **d:** DWI B800) the lesion can be detected well. Despite the high signal in T2w, we could not reliably assign it to the cyst/haemangioma group due to the DWI. With the additional arterial **(e)** and late phase **(f)**, the diagnosis of haemangioma is clear.

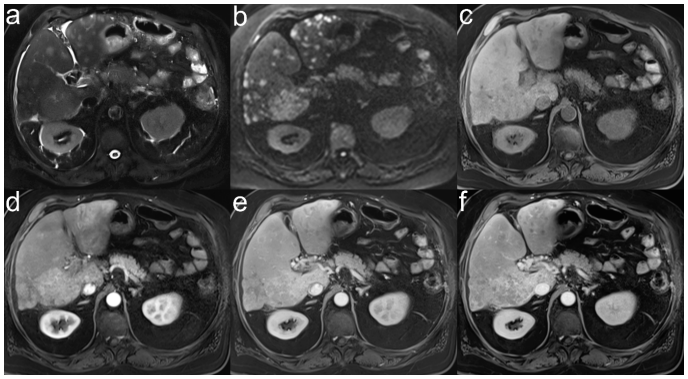


**Figure 4:** 76-year-old patient with multilocular HCC. With the T2w sequence with fat saturation **(a)** and especially the DWI B800 **(b)**, the extent of the disease is easy to recognize, while in the infarction sequences (**c:** native, **d:** arterial phase, **e:** portal venous phase and **f:** late phase) neither the large focus in segment 6 nor the many satellites can be well delineated.

**Table 1:** Sequence parameters of liver MRI.

| | TR, TE (ms) | Matrix | FOV (mm) | Slice thickness | Orientation | b-value |
|---|---|---|---|---|---|---|
| T2w TSE FS | 3700, 100 | 512 x 288 | 400 x 320 | 5 mm | transversal | |
| T2w HASTE FS | 1400, 92 | 256 x 198 | 400 x 325 | 5 mm | transversal | |
| T2w HASTE | 1400, 92 | 256 x 198 | 400 x 325 | 5 mm | transversal | |
| T1w VIBE DIXON | 7.2, 2.4/4.8 | 320 x 156 | 400 x 325 | 5 mm | transversal | |
| DWI FS | 2200, 56 | 268 x 216 | 380 x 306 | 5 mm | transversal | 50, 400, 800 |
| T2w HASTE | 1100, 119 | 320 x 320 | 450 x 450 | 5 mm | coronal | |
| **Contrast media injection** | | | | | | |
| T1w VIBE DIXON art., pv, delayed | 7.2, 2.4/4.8 | 320 x 156 | 400 x 325 | 5 mm | transversal | |
| T1w FLASH FS | 200, 7,2 | 256 x 208 | 400 x 325 | 5 mm | transversal | |
| T1w VIBE DIXON | 6.7, 2.4/4.8 | 288 x 259 | 450 x 450 | 5 mm | coronal | |

TSE: Turbo spin echo; HASTE: Half fourier single shot turbo spin echo; VIBE; Volumetric interpolated breath hold examination; DWI; Diffusion weighted imaging; FLASH: Fast low angle shot; FS: Spectral fat saturation; ART: Arterial phase; PV: Portal venous phase; delayed: delayed phase.

**Table 2:** Signal characteristics of benign and malignant liver lesions in native MR seuqences.

| Lesion | T1w | T2w | DWI b50 | DWI b800 | In/out-of-phase |
|---|---|---|---|---|---|
| Metastasis | Hypointense(-) | Hyperintense (+) (lower signal than CSF). | + | + | / |
| HCC | Isointense(iso) to surrounding liver tissue | iso/+ | + | + | / |
| Cyst// Hemangioma | -/iso // - | Strongly hyperintense (++) // +/similar signal as CSF | ++ | iso/+ | / |
| FNH | -/iso to the surrounding liver tissue | iso/+ and hyperintense central scar | + | iso/+ | / |
| Adenoma | iso to surrounding liver tissue/ + | + | + | iso/+ | Signal drop in the opposed-phase sequence |

**Table 3:** Comparison of liver lesion assignment according to original findings and after 1st and 2nd analysis of native sequences of 240 patients with clinical data.

| Group | Original findings | 1. Native analysis | 2. Native analysis |
|---|---|---|---|
| 1 - No lesion | 84 | 90 | 90 |
| 2 - Metastasis | 61 | 61 | 61 |
| 3 - HCC | 42 | 27 | 33 |
| 4 - Cyst/hemangioma | 27 | 22 | 25 |
| 5 - FNH | 5 | 3 | 3 |
| 5 - Adenoma | 2 | 1 | 2 |
| 6 - other | 19 | 36 | 26 |
| Total | 240 | 240 | 240 |

**Table 4:** Number of patients with 1 to ≥5 detected lesions in group 2 (metastasis), group 3 (HCC), group 4 (cyst/hemangioma), and group 5 (FNH/adenoma) after evaluation of all sequences (native+CM corresponds to original findings), and after reporting of native sequences only (native).

| | Metastasis | | HCC | | Cyst/hemangioma | | FNH | | Adenoma | |
|---|---|---|---|---|---|---|---|---|---|---|
| | Native+CM | Native | Native+CM | Native | Native+CM | Native | Native+CM | Native | Native+CM | Native |
| 1 lesion | 17 | 17 | 15 | 13 | 12 | 10 | 5 | 3 | - | - |
| 2 lesions | 7 | 7 | 12 | 10 | 6 | 6 | - | - | - | - |
| 3 lesions | 6 | 6 | 4 | 0 | 1 | 1 | - | - | - | - |
| 4 lesions | 1 | 1 | 1 | 0 | 1 | 1 | - | - | - | - |
| ≥5 lesions | 43 | 43 | 7 | 5 | 15 | 15 | - | - | 2 | 2 |

**Table 5:** Number of HCC lesions found with all sequences (native+CM) and exclusively the native sequences divided into LI-RADS categories.

| n | LR-3 | LR-4 | LR-5 | Total |
|---|---|---|---|---|
| native + CM | 35 | 26 | 29 | 90 |
| native | 22 (63%) | 13 (50%) | 23 (79%) | 58 (64%) |

**Table 6:** Sensitivity (SE), specificity (SP), positive predictive value (PPV), negative predictive value (NPV), and accuracy of the evaluation of the native MRIs divided into the groups of no lesion, metastasis, HCC, cyst/hemangioma, and FNH/adenoma.

| | SE (%) | SP (%) | PPV (%) | NPV (%) | Accuracy (%) |
|---|---|---|---|---|---|
| No lesion (group 1) | 100 | 96 | 93 | 100 | 98 |
| Metastasis (Group 2) | 100 | 100 | 100 | 100 | 100 |
| HCC (Group 3) | 79 | 100 | 100 | 96 | 96 |
| Cyst/ hemangioma (group 4) | 93 | 100 | 100 | 99 | 99 |
| FNH/ Adenoma (Group 5) | 71 | 100 | 100 | 99 | 99 |

## Discussion

The aim of this study was to determine whether CM is needed for imaging liver lesions and for which indications. Patients with liver lesions were divided into 5 groups. One extra group were patients without liver lesions.

In the "liver metastasis group" we could not detect any advantage regarding the detection and number of liver metastases with additional performance of CM sequences. Using our diagnostic criteria with hypointensity in T1w, hyperintensity in T2w, and diffusion restriction we succeeded in detecting and correctly assigning all liver metastases of the 61 patients with analysis of the native sequence only. Our observation is in agreement with the work of Lavelle et al. [9]. In 2015, they found no advantage of CM sequence over DWI in the hepatobiliary phase in 22 patients with liver metastases from neuroendocrine tumours and concluded that DWI is an adequate tool for visualization and assessment of neuroendocrine metastases in clinical applications. Also, Allam et al. [10] (2017) found no advantage of CM sequences regarding the detection of metastases compared to DWI when studying 20 patients (15 with multiple and 5 with isolated liver metastases). In contrast to our work, Allam et al. included the ADC value in their evaluation and defined all ADC values below 0.8 x $10^{-3}$ $mm^2$ /s as malignant. The ADC value was not included in our study because respiratory motion does not always ensure an identical depth of breath at b50 and b800, and the ADC value, especially in small lesions, could be calculated incorrectly by consequence. Instead, we used the lack of signal drop between the low and high b values as a diagnostic criterion. Also, Hwang et al. [11] showed in their study that native liver MRI can be used as an alternative to gadoexatic acid-enhanced liver MRI in the detection of liver metastases from colorectal cancer.

Chung et al. [12] reported that it is difficult to distinguish very small metastases from vessels using CM sequences. In these cases, DWI has the great advantage because it effectively suppresses the signal from vessels above a b value of 50 [13]. In the present evaluation, we were able to detect 16 liver metastases with a size of ≤1.0 cm in 5 patients using DWI. Thus, DWI represents the crucial sequence for the detection of liver metastases. Also, good image quality of DWI with complete coverage of the liver without gaps is important. Therefore, image acquisition should be measured in free breathing with breath triggering. One problem, however, is occasionally the left lobe of the liver, where extinction phenomena may occur due to proximity to the heart (Figure 2). This can be overcome by flow-compensated DWI [14].

The perfusion behaviour of liver metastases may give an indication of the primary tumour. Liver metastases, e.g., from lung, colon, or gastric carcinomas, are often hypovascular in the arterial phase, whereas metastases from NET, renal cell carcinoma, or thyroid carcinoma are often hypervascular [15]. Consequently, we could not use the native sequences alone to infer the primary tumour. Despite this limitation, according to our results, the native sequence is a very good method for the detection of liver metastases.

After ablation therapy, delineation of the defect and assessment of residual tumour tissue in native technique may be difficult. In the present study, 12 patients with liver metastases had received ablation therapy. Ablation treatments can lead to periablation edema and signal changes in the high b values (B800), especially in the initial follow-up, after therapy [16]. Therapeutically induced tissue changes (e.g., necrosis, periablation edema, fibrosis, inflammatory responses) are associated with lower signal intensities compared with tumour tissue in the high b values and hyperintensity in the ADC map. In contrast, tumour tissue is hyperintense in high b values and hypointense in ADC. In one patient from our collective, we found 3 metastasis-selective lesions at one large ablation defect and one metastasis-selective lesion at another ablation defect due to the high signal in the high b-value DWI. However, with purely native sequences, it is occasionally difficult to identify the location and size of the ablation defect. In our study, we could not confidently assign 5 lesions with the native sequences that could be clearly assigned to ablation defects with i.v. CM. Therefore, the first follow-up after an ablative procedure should be performed with i.v. CM.

In the cyst or hemangioma group, 101/106 lesions were diagnosed as cyst or hemangioma in 22/27 patients with native imaging only. The diagnostic criterioin for both entities was a lesion that was hypo-/isointense in T1w, severely hyperintense in T2w, and iso-/hyperintense with high b-values [17,18]. Since we had no discriminator for cyst versus hemangioma with the native sequences, we could not confidently distinguish between the two entities in any of the patients. In individual cases, it may be difficult to diagnose cyst/hemangioma with certainty using only native sequences. In our collective, 2 patients (1 cyst/1 hemangioma) had abnormal lesions detected on MRI that we could not confidently assign to a cyst/hemangioma using only native sequences (Figure 3). Therefore, at least one MRI with i.v. CM should be performed in every patient to exclude malignant liver lesions or to further clarify suspicious liver lesions in other imaging modalities. In individual cases, differentiation between cystic metastases and simple cysts may be difficult. After evaluation of our data, all metastases were correctly identified, so no cystic metastasis was misclassified as a simple cyst. Fifteen of 16 cysts in our collective were homogeneous in T1 and T2 weighting and without fluid-fluid levels, which is why they were classified as cysts. The two relevant factors for differentiation are a strong hyperintense signal behaviour of the cyst in T2w and DWI with low b value and a decreasing signal in DWI with high b value. In contrast, metastases are diffusion impaired with hypointensity in ADC and strong signal in DWI at high b values. Vaccha et al. [19] described simple cysts as homogeneous in T1w and T2w. In contrast, cystic metastases had wall irregularities, wall thickening, septation, hemorrhage or contrast enhancement, and diffusion defects, as well as a stratification phenomenon as diagnostic criteria.

In the HCC group, 48 of 90 lesions were diagnosed as HCC in 27 of 42 patients with native imaging only. The diagnostic criterion was an iso-/hyperintense lesion in T1w with diffusion abnormality in patients with liver cirrhosis [20,21]. Also, Gluskin et al. [22] reported in 2015 that in HCC patients in whom contrast administration was not possible, DWI can be very helpful in detecting HCC lesions. In our study, 2 patients with HCC had very weak CM enhancement and were not reliably detected as HCC without DWI (Figure 4). In 3 patients with HCC, lesions with diffusion restriction without CM uptake were found in the arterial phase. Only during follow-up all of these lesions showed CM uptake. DWI was more sensitive than CM sequences in these cases and one should consider including DWI in the LI-RADS criteria [8]. Interestingly,

the detection rate of HCC foci with high LI-RADS classification was not better than with low LI-RADS classification. In summary, our results show that CM sequences are necessary for reliable detection of HCC lesions, but DWI can be helpful in individual cases. In a study of 50 HCC patients treated by radioembolization, DWI also showed in isolated cases an advantage over Gd-EOB-DTPA MRI with respect to therapy evaluation [23].

In our collective, 5/240 patients had FNH and 2/240 patients had liver adenoma. Our diagnostic criteria for FNH were according to Bieze et al. [24] a hypo-/isointense lesion in T1w, a hyperintense central scar in T2w, and an iso-/mildly hyperintense lesion in DWI/ADC, and for a liver adenoma according to Ronot et al. [25] an iso-/hyperintense lesion in T1w with a signal drop in the opposed phase, due to fat content, which is slightly hyperintense to the surrounding liver tissue in T2w and in DWI. Using these diagnostic criteria, we were able to correctly match 3 of 5 patients with one FNH lesion each and 1/2 patients with ≥5 liver adenomas each using native imaging only. After the 2nd native analysis, we were also able to correctly group the other patient with liver adenomas using the preliminary images. The remaining 2/5 patients with FNH did not show hyperintense central scar in T2w, thus their correct assignment was not possible. With a sensitivity of 71%, native MRI is thus not suitable to detect liver adenoma or FNH. Assignment of these entities is often only possible with MRI using liver-specific contrast agents [17] and is important, as liver adenomas can malignantly degenerate and/or hemorrhage in the liver [26,27].

In 36 of 240 patients, 54 lesions were found in native technique that could not be assigned to groups 1 to 5 using our criteria. After a 2nd analysis with the aid of the previous findings, the previous images, and the electronic medical record, this was successful in 16 of 36 patients (HCC (n=6), hemangioma (n=3), adenoma (n=1), CCC (n=4), NEC of the gallbladder (n=1), and epithelioid hemangioendothelioma (n=1)).

The remaining 20 patients could not be further classified. These were patients with an HCC (n=3), cyst (n=1), hemangioma (n=1), FNH (n=2), CCC (n=1), ablation defect (n=5), and angiosarcoma (n=1). Six patients had a lesion that could not be confidently assigned to an entity, even with the use of contrast sequences, or histologic confirmation was not performed. The lesions in these 20 patients can be divided into two groups. First, lesions that can be detected better with CM than with the native sequences including DWI. These include ablation defects (n=5), CCC (n=1), and atypical cyst with less signal in T2w (n=1). On the other hand, lesions showing particular CM dynamics such as hemangioma (n=1) and HCC (n=3).

### Limitations

The current study is subject to certain limitations. The small number of lesions (n=498), especially the small number of FNHs and adenomas, and the retrospective study design might have influenced the statistical results. Our result with a sensitivity and specificity of 100% of native sequences for metastases would probably be slightly worse with a larger number of metastases (n=268). Nevertheless, DWI has a very good sensitivity for liver metastases, which cannot be improved by non-liver specific contrast medias. In a few other studies [28,29], sensitivity for metastases was slightly increased with liver-specific contrast agents.

MRI findings with i.v. CM and native sequences including DWI were chosen as the reference standard. Histopathologic findings of the lesions were available only in isolated cases, whereas an incorrect classification of the lesions in the reference standard should be negligible. At our institute, DWI has a high value for the detection of liver metastases. It is possible that even in the reference standard, the DWI images were the main ones used for diagnosis, while all other sequences, especially those after CM administration, played a minor role.

## Conclusion

In our study, liver MRI with exclusively native sequences was only convincing in the detection of liver metastases. In future, contrast media could be omitted for examinations to follow-up known liver metastases or for the first follow-up examination after an ablative procedure. Even the reliable exclusion of metastases, e.g., preoperatively, would be possible using the native technique. However, this requires a DWI with good image quality. In all other entities, the administration of i.v. contrast media is mandatory at present.

## Declarations

**Note:** The present work has been carried out in (partial) fulfilment of the requirements for the award of the degree of Dr. med.

**Conflict of interest:** Authors declare no conflict of interest.

## References


1. Ba-Ssalamah A, Fakhrai N, Matzek WK, Herneth AM, Stadler A, Bastati N, et al. Magnetic resonance imaging of liver malignancies. Top Magn Reson Imaging. 2007; 18: 445-455.
2. Marrero JA, Ahn J, Rajender Reddy K, Americal College of G. ACG clinical guideline: the diagnosis and management of focal liver lesions. Am J Gastroenterol. 2014; 109: 1328-1347; quiz 1348.
3. Mao Y, Chen B, Wang H, Zhang Y, Yi X, Liao W, et al. Diagnostic performance of magnetic resonance imaging for colorectal liver metastasis: A systematic review and meta-analysis. Sci Rep. 2020; 10: 1969.
4. Shamam YM, De Jesus O. Nephrogenic Systemic Fibrosis In. StatPearls Publishing Copyright © 2023, StatPearls Publishing LLC. 2023;
5. Guo BJ, Yang ZL, Zhang LJ. Gadolinium Deposition in Brain: Current Scientific Evidence and Future Perspectives. Front Mol Neurosci. 2018; 11: 335.
6. Fischbach F, Fischbach K. MRT der Leber. 1st edn. Stuttgart: Thieme. 2017.
7. Nalaini F, Shahbazi F, Mousavinezhad SM, Ansari A, Salehi M. Diagnostic accuracy of apparent diffusion coefficient (ADC) value in differentiating malignant from benign solid liver lesions: a systematic review and meta-analysis. BR J Radiol. 2021; 94: 20210059.
8. Moura Cunha G, Chernyak V, Fowler KJ, Sirlin CB. Up-to-Date Role of CT/MRI LI-RADS in Hepatocellular Carcinoma. J Hepatocell Carcinoma. 2021; 8: 513-527.
9. Lavelle LP, O'Neill AC, McMahon CJ, Cantwell CP, Heffernan EJ, Malone DE, et al. Is diffusion-weighted MRI sufficient for follow-up of neuroendocrine tumour liver metastases? Clin Radiol. 2016; 71: 863-868.

10. Allam KE, Shalaby MH, Moulood IA. Role of Diffusion Weighted MRI Imaging in Detection of Liver Metastasis. The Egyptian Journal of Hospital Medicine. 2017; 69: 1823-1827.

11. Hwang JA, Kim YK, Min JH, Song KD, Sohn I, Ahn HS. Non-contrast liver MRI as an alternative to gadoxetic acid-enhanced MRI for liver metastasis from colorectal cancer. Acta Radiol. 2019; 60: 441-450.

12. Chung WS, Kim MJ, Chung YE, Kim YE, Park MS, Choi JY, et al. Comparison of gadoxetic acid-enhanced dynamic imaging and diffusion-weighted imaging for the preoperative evaluation of colorectal liver metastases. J Magn Reson Imaging. 2011; 34: 345-353.

13. Holzapfel K, Schreyer AG. Diffusionsgewichtete MRT des Abdomens. Radiologie up2date. 2020; 20: 219-232.

14. Laun FB, Fuhres T, Seuss H, Muller A, Bickelhaupt S, Stemmer A, et al. Flow-compensated diffusion encoding in MRI for improved liver metastasis detection. Plos one. 2022; 17: e0268843.

15. Namasivayam S, Martin DR, Saini S. Imaging of liver metastases: MRI. Cancer Imaging. 2007; 7: 2-9.

16. Schraml C, Schwenzer NF, Clasen S, Rempp HJ, Martirosian P, Claussen CD, et al. Navigator respiratory-triggered diffusion-weighted imaging in the follow-up after hepatic radiofrequency ablation-initial results. J Magn Reson Imaging. 2009; 29: 1308-1316.

17. Topp S, Aissa J, Quentin M. Fokale Leberläsionen. Schultheis KH, Mödder U, Antoch Gs. In. Thieme. 2018;

18. Mamone G, Di Piazza A, Carollo V, Cannataci C, Cortis K, Bartolotta TV, et al. Imaging of hepatic hemangioma: from A to Z. Abdom Radiol (NY). 2020; 45: 672-691.

19. Vachha B, Sun MR, Siewert B, Eisenberg RL. Cystic lesions of the liver. AJR Am J Roentgenol. 2011; 196: W355-366.

20. Schreyer AG, Lüth S, Ringe KI. Bildgebung in der zirrhotischen Leber – warum, wie und was ist LI-RADS? Radiologie up2date. 2022; 22: 69-84.

21. Lincke T, Boll D, Zech C. Bildgebung des hepatozellulären Karzinoms. Radiologie up2date. 2016; 16: 295-310.

22. Gluskin JS, Chegai F, Monti S, Squillaci E, Mannelli L. Hepatocellular Carcinoma and Diffusion-Weighted MRI: Detection and Evaluation of Treatment Response. J Cancer. 2016; 7: 1565-1570.

23. Schelhorn J, Best J, Reinboldt MP, Dechene A, Gerken G, Ruhlmann M, et al. Does diffusion-weighted imaging improve therapy response evaluation in patients with hepatocellular carcinoma after radioembolization? comparison of MRI using Gd-EOB-DTPA with and without DWI. J Magn Reson Imaging. 2015; 42: 818-827.

24. Bieze M, van den Esschert JW, Nio CY, Verheij J, Reitsma JB, Terpstra V, et al. Diagnostic accuracy of MRI in differentiating hepatocellular adenoma from focal nodular hyperplasia: prospective study of the additional value of gadoxetate disodium. AJR Am J Roentgenol. 2012; 199: 26-34.

25. Ronot M, Bahrami S, Calderaro J, Valla DC, Bedossa P, Belghiti J, et al. Hepatocellular adenomas: accuracy of magnetic resonance imaging and liver biopsy in subtype classification. Hepatology. 2011; 53: 1182-1191.

26. Stoot JH, Coelen RJ, De Jong MC, Dejong CH. Malignant transformation of hepatocellular adenomas into hepatocellular carcinomas: a systematic review including more than 1600 adenoma cases. HPB (Oxford). 2010; 12: 509-522.

27. Mohajer K, Frydrychowicz A, Robbins JB, Loeffler AG, Reed TD, Reeder SB. Characterization of hepatic adenoma and focal nodular hyperplasia with gadoxetic acid. J Magn Reson Imaging. 2012; 36: 686-696.